Wind Estimations with Meteor Observations by MF Radars at Poker Flat, Alaska and Wakkanai, Japan

KAWAMURA Seiji, TSUTSUMI Masaki, and MURAYAMA Yasuhiro

A new measurement mode is introduced into two MF (medium frequency) radars of NICT at Wakkanai and Poker Flat, Alaska in August 2004. In this method, meteor trails are used to estimate wind velocities. The positions of meteor trails are determined by the interferometry technique, and horizontal wind velocities are estimated by their line-of-sight Doppler velocities. The height coverage of this technique by MF radars is from about 80 to 120 km. Wind velocities by meteors show quite good agreement with those by FCA technique (a traditional method to estimate winds by MF radar). In this paper, a method and observed results are reported.

Keywords
MF radar, Meteor, Wind velocity, Mesosphere and lower thermosphere

1 Introduction

The earth's atmosphere and its climate are highly dependent on the altitude. Interactions and coupling processes between different altitude regions are still important subjects to be revealed. The features of the earth's atmosphere below and above 100 km altitude are especially different. The neutral atmospheric processes are dominant in the lower region, while the upper region is strongly affected by the condition of outer space. To be able to understand the relationship between the earth's atmosphere and the space environment, information on the atmosphere at around 100 km altitude, which corresponds to the transition region, is extremely important. MF radar enables continuous measurements of horizontal wind velocity and electron density at altitudes of approximately 60–90 km, and is regarded as among the most powerful tools for observation of the mesosphere and lower thermosphere (MLT) region. Estimation of horizontal wind velocity is performed using a method known as FCA (Full Correlation Analysis), based on the motion of turbulence structure in the atmosphere[1]. The wind measurement performance of the FCA method at altitudes below 90 km has been verified through comparative studies with other observation techniques, but above 90 km, the FCA method is known to result in large errors in estimation[2]. Since the MF radar FCA method cannot cover the altitude range of 90–120 km (which overlaps the above-mentioned transition region), meteor radars that make use of the HF and VHF bands are used for wind velocity measurements in this region. On the other hand, Tsutsumi et al. [1999] have demonstrated that horizontal wind velocity observations can be made using meteor observation by MF radars that make use of the medium frequency band[3]. Thus, the MF radar at Showa Station, Antarctica, is currently used for horizontal wind velocity observation utilizing both the FCA method and meteor observation[4].

NICT has deployed MF radars at three

sites: Wakkanai, Yamagawa, and Poker Flat, Alaska, for continuous observation of horizontal wind velocity and electron density. Table 1 presents the main specifications of these radars. Of the three sites, horizontal wind estimation based on meteor observation has been underway since August 2004 at Poker Flat and Wakkanai, where no changes to the hardware (such as antenna configuration) were required for additional meteor observations. The present paper will introduce the procedures of wind velocity observation based on meteor observation, which was newly added to the functions of NICT's MF radar, using the Poker Flat MF radar as an example.

2 Method of wind observation using meteors

Let us first provide an outline of wind velocity estimation based on meteor observation. When meteors penetrate the earth's atmosphere, they ionize the surrounding atmosphere as they push their way through it, and ultimately disintegrate. The bar-shaped trail formed along the meteor's path drifts along with the background wind before it is scattered by dispersion or recombination. By observing this plasma with radar and calculating the meteor position and the Doppler shift, it is possible to determine the velocity component of the plasma in the direction of the meteor trail relative to the radar (i.e., along the line-of-sight). This velocity may be regarded as the line-of-sight component of the background wind velocity. Since multiple line-of-sight wind velocities can be obtained by observing multiple meteors in a given space and time, the horizontal wind velocity may be estimated by fitting, assuming that the vertical wind component is sufficiently small. Since interferometric techniques are required to determine meteor position, an array of multiple antennas must be installed and properly arranged.

The meteor echo can be categorized into

Table 1 *Main specifications of the MF radar of NICT*

Site (Lat., Long.)	Yamagawa, Japan (31.20 N, 130.62 E)	Wakkanai, Japan (45.36 N, 141.81 E)	Poker Flat, Alaska (65.1 N, 147.5 W)
Frequency	1.9550 MHz	1.9585 MHz	2.43 MHz
Bandwidth	60 kHz (24 kHz since Sept. '96)	24 kHz	60 kHz
Peak Power	50 kW	50 kW	50 kW
Pulse duration	27 μs (48 μs since Sept. '96)	48 μs	27 μs
Time resolution	4 min.	4 min. (6 min. since Aug. '04)	3 min. (5 min. since Aug. '04)
Range resolution	7 km	7 km	4 km
Sampling interval	2 km	2 km	2 km
Antenna	Tx: 4 dipoles Rx: 3 cross-dipoles	4 cross-dipoles (for Tx and Rx)	4 cross-dipoles (for Tx and Rx)
Observation	FCA since Sept. '94 DAE since Sept. '98	FCA & DAE since Sept. '96 MET since Aug. '04	FCA since Oct. '98 DAE since Nov. '97 MET since Aug. '04

FCA: wind velocity measurement mode by Full Correlation Analysis,

DAE: electron density measurement mode by Differential Absorption Experiment,

MET: wind velocity measurement mode by meteor obserbation.

an over-dense echo or an under-dense echo, based on the relationship between the plasma frequency of the meteor-generated plasma and the frequency of the radar radio wave. When the plasma frequency is higher than the frequency of the radio wave, an over-dense echo is created, and the radio wave is fully reflected at the surface of the bar-shaped plasma (total reflection). Since the Doppler shift in this case will correspond to the velocity at which the bar-shaped plasma is expanding in the radial direction and not to the background wind velocity, the over-dense echo cannot be used to estimate wind velocity. Thus, background wind velocity can only be estimated based on the under-dense echo returned from the bar-shaped plasma in which radio waves can propagate.

The basic flow of the wind velocity estimation process based on meteor observation is as follows.

a. Inter-channel phase and amplitude calibrations of the received signals
b. Detection of meteors from the received data
c. Positional determination of meteors
d. Wind velocity estimation

2.1 Inter-channel phase and amplitude calibrations of received signals

Figure 1 shows the antenna configuration of the Poker Flat MF radar. Cross dipoles have been set at four positions—the apexes and the center of an equilateral triangle—to form four channels (CH 1–4). In order to make a precise determination of meteor position by interferometry and to improve the precision of meteor detection by offline beam formation (as will be described later), the signals received by each of these four channels must be calibrated so that they will feature the same phase and amplitude.

Figure 2 is a plot of the inter-channel phase difference using CH 4 as the standard channel. The data utilized were acquired by FCA observation during the 10-day period from Aug. 1–10, 2004. It can be seen from the top panels that the variations in phase differences increase at higher altitudes. This is due to the effects of meteor echoes. Here, phase calibration will be performed only on data at low altitudes (below 70 km) where the effects of meteors may be considered negligible (i.e., where only the effects of partial reflection from the atmosphere in the zenithal direction are present). The bottom panels are histograms of the phase difference of data only from altitudes below 70 km. The Gaussian curve determined by fitting is shown by the red lines; based on these lines, the relative phase differences of CH 1, CH 2, and CH 3 relative to CH 4 were calculated at 77.9°, 83.1°, and 17.0°, respectively. Figure 3 shows similar plots for amplitude, except that in these cases, CH 1 is used as the standard for the amplitude ratios. For phase difference, only data from altitudes below 70 km were used to plot the histogram (bottom panels); the results of fitting showed that the amplitude ratios of CH 2, CH 3, and CH 4 relative to CH 1 were 1.089, 0.931, and 0.607, respectively.

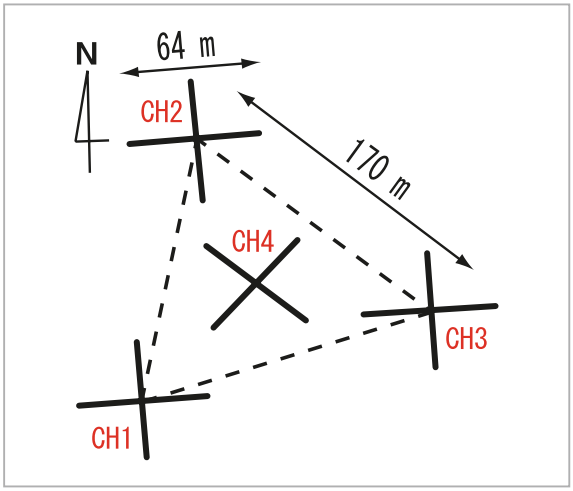

Fig. 1 *Antenna configuration of Poker Flat MF radar*

2.2 Meteor detection from received signal data

The time and spatial resolution of the wind velocity estimation using meteors can be improved by increasing the number of meteors to the full extent possible. This increase will also result in more precise estimation. Accord-

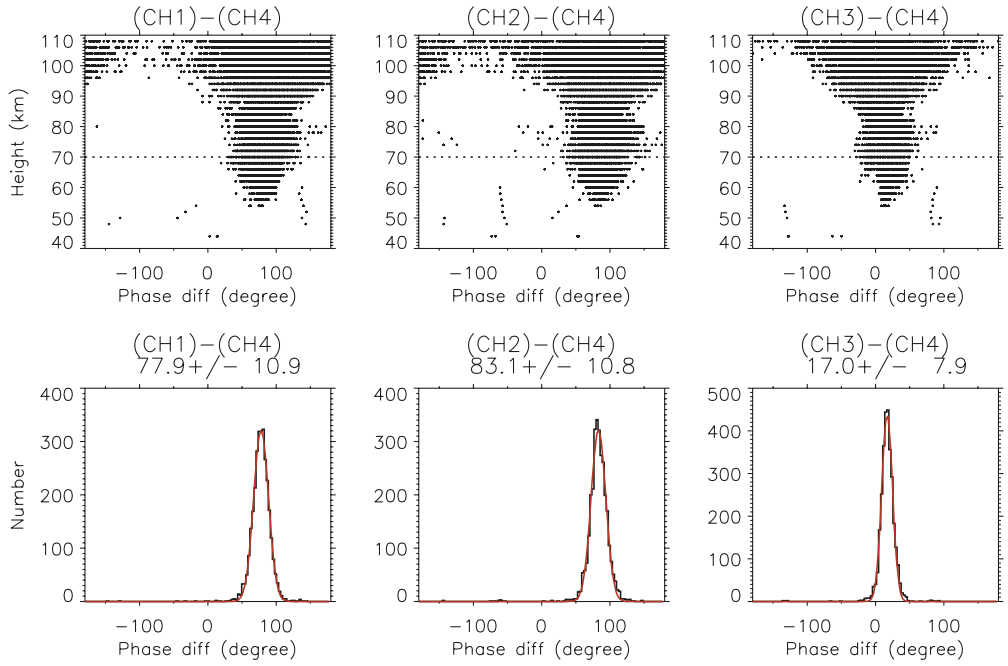

Fig.2 *Distribution of phase difference for each channel*

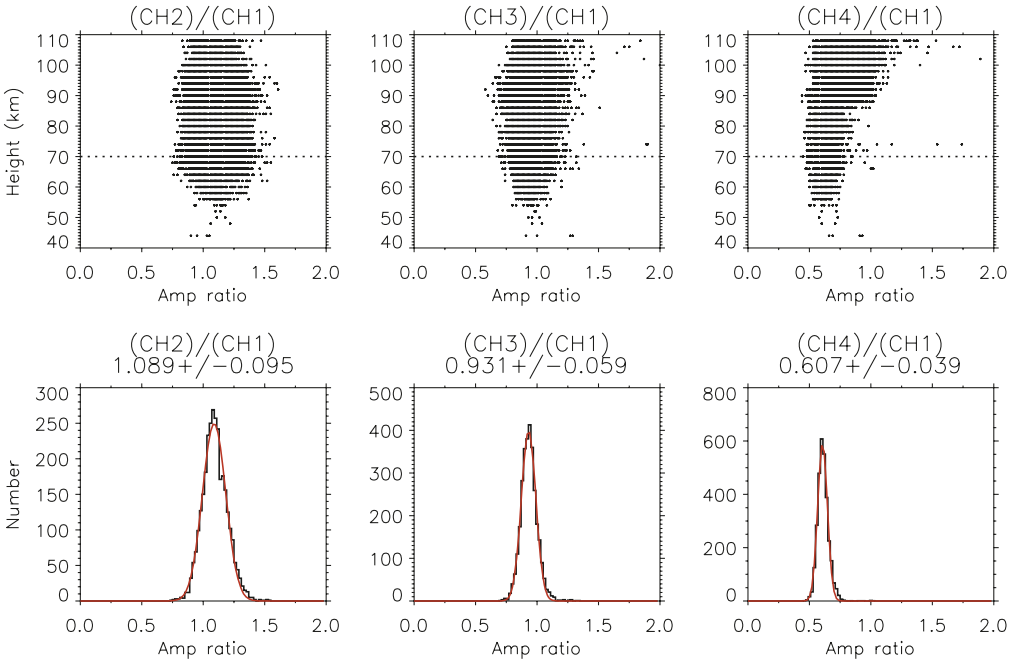

Fig.3 *Distribution of amplitude ratio for each channel*

ingly, we arranged to enable meteor detection other than near the zenithal direction through offline beam formation. Figure 4 presents a schematic view of the procedure. The signals received for the four channels are combined by shifting the phase of each. This is equivalent to forming a beam slanted approx. 25° off-axis from the original one, even

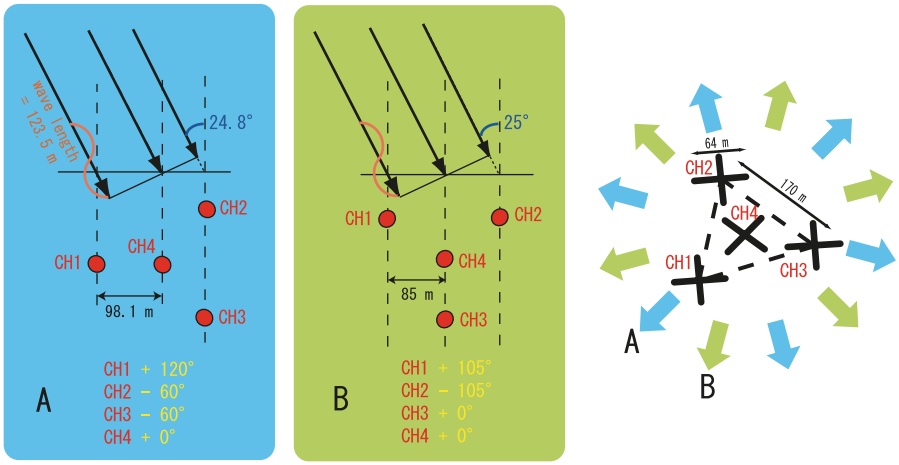

Fig.4 *Schematic diagram of offline beam formation for meteor detection*

though this phase shift is performed after the signals are received. By combining the signals from each channel by providing phase differences, as shown in Fig. 4A, a beam is formed that slants 24.8° in the direction of blue arrow A in the illustration in the right-hand side of Fig. 4. The same phase difference pattern may be provided to form beams in the six directions indicated by the blue arrows. By using the phase difference pattern shown in Fig. 4B, beams slanted 25° in the directions shown by the green arrows may be formed. The twelve beams formed in this manner, in addition to the beam in the zenith direction (the original radar beam), are used to perform meteor detection.

Figures 5 and 6 present examples of meteor detection using received time series data. Figure 5 plots the time series of power (left panels) and phase (right panels) for the signals received by CH 1 through CH 4, from top to bottom, respectively. Although slightly different patterns are observed near the end of the time series for the phase (near the right-hand side of the plot), it is difficult to identify meteor trails from the raw signal power data alone. Figure 6 presents the time series of the synthesized signal created by applying phase differences to the four received signals (offline beam formation). At this point the meteor echo is clearly visible in the red hatched area.

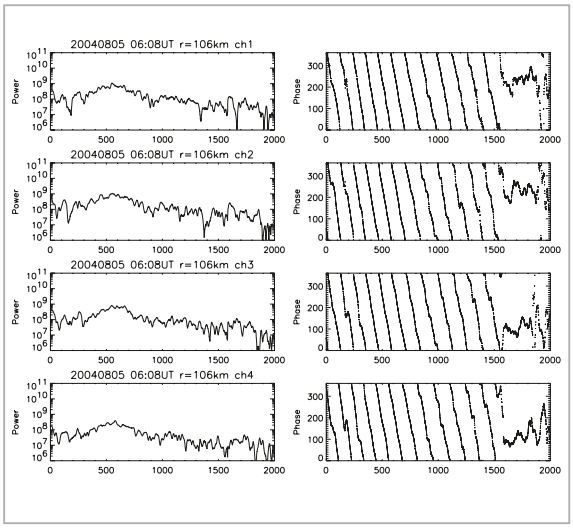

Fig.5 *Time series of signal power (left) and phase (right) for each channel*

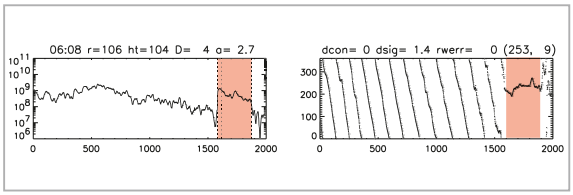

Fig.6 *Meteor echo visualized by offline beam formation*

Because multiple virtual beams are created in an offline beam formation, it is possible that a single meteor may be detected by multiple beams. It therefore becomes necessary to identify meteors that are located near each other in space and time, and to consider these identi-

fied meteors as identical, to prevent duplication of data.

2.3 Meteor position determination

The position of a meteor can be determined using interferometric techniques using the phase of the signals received by each antenna, in accordance with the configuration shown in Fig. 1. This is why phase calibration is performed at the beginning of data processing. Of the multiple baselines constituting the interferometer, data from the longest baseline will have the highest precision in meteor positioning. However, it is also possible that the meteor position cannot be uniquely determined when the shortest baseline is not less than the half-wavelength of the transmitted radio wave. In the case of the Poker Flat MF radar, the longest baseline is 170 m (one side of the equilateral triangle) and the shortest baseline is 98.1 m (distance from the center to the apex antenna). Since the shortest baseline is longer than the half-wavelength (61.7 m) of the transmitted radio wave, multiple candidates may possibly appear in the determination of meteor position. In such a case, the final judgment on the meteor position is made based on conditions such as the realistically estimated altitude of the meteor trail.

2.4 Wind velocity estimation

After the meteor is detected and its position successfully determined, the next step is to calculate the Doppler shift of the meteor echo based on a time series of the phase. The Doppler shift determined here corresponds to the component in the direction of the straight line connecting the radar and the meteor (line-of-sight component) of the velocity of the meteor trail drifting with the background wind. Thus, the line-of-sight component of the background wind at the point of the meteor can be determined for each meteor. By detecting multiple meteors within a given window of space and time and fitting the results of the line-of-sight wind velocity components, the representative wind velocity for the window can be calculated. In this calculation, the vertical wind component is considered to be sufficiently small compared to the horizontal component and is thus ignored. The temporal and spatial resolutions of wind velocity are dependent on the range of space and time of the meteors employed in the calculation. Thus, by detecting higher numbers of meteors, resolution, as well as the precision of wind estimation, can be improved.

3 Meteor distribution

Before presenting the wind velocity estimated by meteor observation, in this section we will examine the meteor distribution detected under this method. Figure 7 presents the distributions of meteors detected during a 24-hour period on Aug. 24, 2004. On this day, 1,398 meteors were detected within the full period of observation. From left to right at top are the LT (local time) distribution, range distribution, and height distribution, respectively, and from left to right on the bottom are zenith angle distribution, azimuth angle distribution, and arrival angle distribution, respectively. The number of meteors displays large diurnal variations, and peaks at dawn. It can be seen from the height distribution that meteors are distributed within ±20 km of approximately 100 km in height. The apparent characteristic pattern in the arrival angle distribution shown in the bottom right of Fig. 7 is believed to be caused by the reflection of the MF radar beam pattern. Figure 8 is an illustration of the beam pattern of the Poker Flat MF radar. Since the radar transmits radio waves from four points at the apexes and center of an equilateral triangle, the synthesized beam will display the pattern shown by the red line. This pattern is consistent with that observed in the arrival angle. However, the half width at half maximum of the MF radar beam is around 30°, and so the 60°-spread in the meteor zenith-angle distribution is considered to result from offline beam formation.

In the example given in Fig. 7, nearly 1,400 meteors were detected in a single day. However, the number of meteors fluctuates

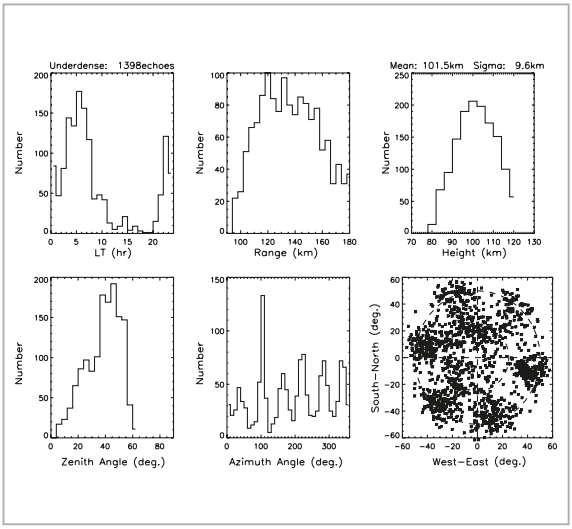

Fig.7 *Distributions of meteors detected for 24 Aug 2004*

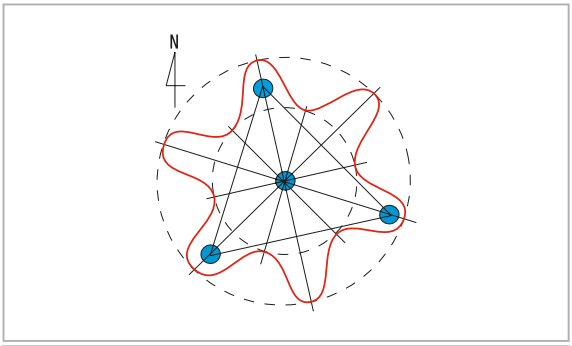

Fig.8 *Beam pattern of the Poker Flat MF radar*

significantly from day to day, and there are days on which only 200 or so are detected. In the month of Aug. 2004, there were a total of approximately 20,000 meteors detected, or an average of 640 per day.

4 Wind velocity estimated from meteors

In this section, we will compare the wind velocities estimated from meteor observations with those measured by the FCA method. At Poker Flat, MR radar observation is alternated between a 2-minute FCA wind velocity observation, 1-minute DAE electron density observation, and 2-minute meteor trail observation. Therefore, the wind velocities observed by the FCA method and by meteors may basically be regarded as having been measured simultaneously. The time and spatial resolutions of the wind velocity estimation using meteors were set at 1 hour and 4 km, respectively. The height resolution of the FCA method is 4 km. Although the time resolution of the FCA method is 5 minutes, 1-hour averages will be used to enable comparison with the wind velocities estimated from meteors.

Figure 9 shows the results of wind velocity estimation for Aug. 24, 2004. From top to bottom, the panels show the distributions of zonal wind calculated from meteor observation (eastward positive), zonal wind by the FCA method, the meridional wind from meteor observation (northward positive), meridional wind by the FCA method, and number of meteors used in the relevant wind velocity estimation. It should be noted that the range of observation height differs for the meteor and FCA methods. In the height range where both methods overlap, the results are fairly consistent between the two methods. It has been pointed out that the wind velocity estimated by the FCA method tends to be smaller than the actual value at altitudes exceeding 90 km. In the present comparison, it can be seen that the wind velocity estimated from meteor observation for zonal winds at 15–20 UT have larger values than the corresponding FCA results. When the winds estimated by the two methods are combined in the height direction, it may be seen that the scale and variation patterns of wind velocity seem to be smoothly connected. Although in certain areas the estimated wind velocity cannot be considered reliable due to insufficient meteor numbers, the results here indicate that the wind velocities estimated from meteor observation are virtually consistent with the results of the FCA method, as long as sufficient numbers of meteors can be detected.

Figure 10 compares the diurnal variations in 1-month averaged wind velocities from Aug. 9 to Sep. 9, 2004. The format is the same as for Fig. 9. It can be seen that for the 1-month average, the results of the two methods display even higher consistency.

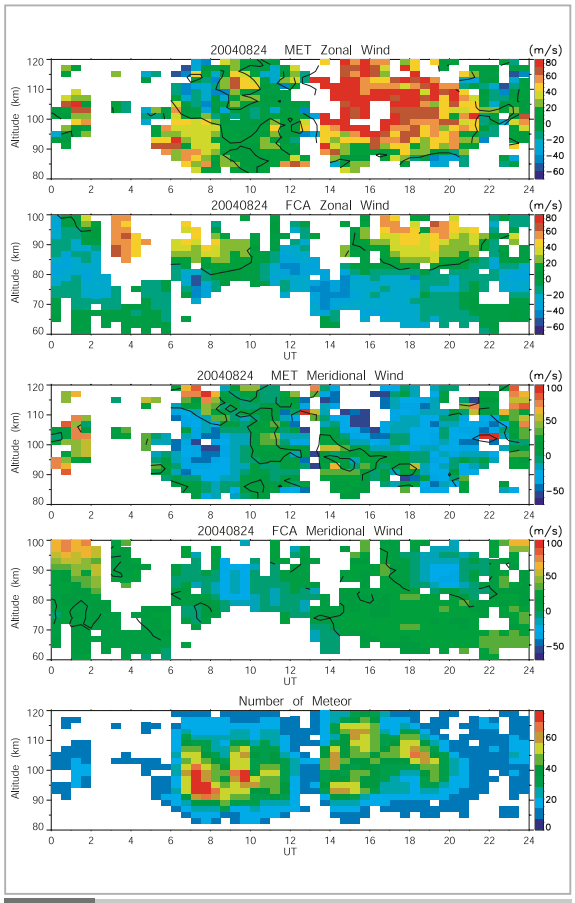

Fig.9 *Comparison of wind velocities estimated from meteor observation and by FCA method*

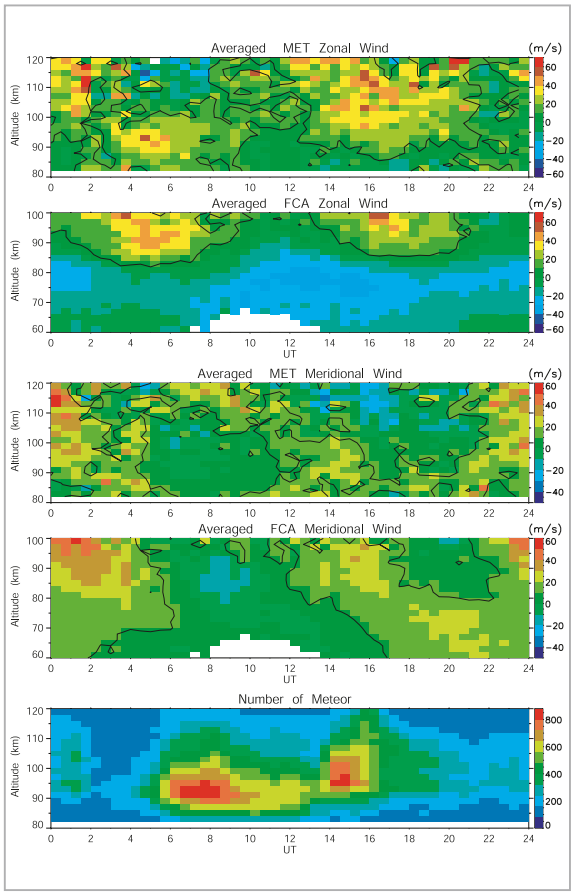

Fig.10 *Comparison of the 1-month averages of wind velocity estimated from meteor observation and by FCA method*

5 Conclusions

Of the three MF radars owned by NICT, the function of wind velocity estimation based on meteor observation was added to those at Wakkanai and Poker Flat, Alaska. In this paper, the Poker Flat MF radar was used as an example to introduce the procedures and observation results of meteor observation using MF radar. In the month of Aug. 2004, there were a total of approximately 20,000 meteors detected, or an average of 640 per day. When sufficient numbers of meteors can be detected, the wind velocities estimated from meteor observations were found to be fairly consistent with the FCA results, which demonstrates that meteor observations can expand the height coverage of wind velocity observation for MF radars.

References

1 B. H. Briggs, “The analysis of spaced sensor records by correlation techniques”, Handbook for MAP, Vol.13, 166-186, 1984.

2 D. A. Holdsworth, “Influence of instrumental effects upon the full correlation analysis”, Radio Sci.,34, 643-655, 1999.

3 M. Tsutsumi, D. Holdsworth, T. Nakamura, and I. Reid, “Meteor observations with an MF radar”, Earth Planets Space, 51, 691-699, 1999.

4 M. Tsutsumi and T. Aso, “MF radar observations of meteors and meteor-derived winds at Showa (69S, 39E), Antarctica: A comparison with simultaneous spaced antenna winds”, J. Geophys. Res., Vol.110, D24111, doi:10.1029/2005JD005849, 2005.

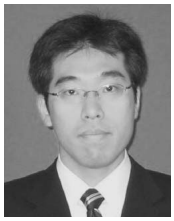

***KAWAMURA Seiji**, Ph.D.*

Researcher, Environment Sensing and Network Group, Applied Electromagnetic Research Center

Atmospheric Physics, Radar Engineering

***TSUTSUMI Masaki**, Ph.D.*

Associate Professor, National Institute of Polar Research

Atmospheric Physics

***MURAYAMA Yasuhiro**, Dr. Eng.*

Planning Manager, Strategic Planning Office, Strategic Planning Department

Dynamics in the Thermosphere and Mesosphere